JVST A
Journal of Vacuum Science & Technology A

ARTICLE

pubs.aip.org/avs/jva

Film and surface stress during Al_2O_3 thermal atomic layer etching using *in situ* wafer curvature measurements

Cite as: J. Vac. Sci. Technol. A **44**, 032605 (2026); doi: 10.1116/6.0005425
Submitted: 21 February 2026 · Accepted: 2 April 2026 ·
Published Online: 28 April 2026

View Online Export Citation CrossMark

Ryan B. Vanfleet,[1] Victor M. Bright,[2] and Steven M. George[1,a)]

AFFILIATIONS

[1]Department of Chemistry, University of Colorado, Boulder, Colorado 80309
[2]Department of Mechanical Engineering, University of Colorado, Boulder, Colorado 80309

Note: This paper is part of the Special Topic on Atomic Layer Etching (ALE).
[a)]**Electronic mail:** Steven.George@Colorado.edu

ABSTRACT

In situ wafer curvature measurements were employed to monitor film and surface stress during Al_2O_3 thermal atomic layer etching (ALE). The Al_2O_3 thermal ALE was performed using fluorination and ligand-exchange reactions using sequential hydrogen fluoride (HF) and trimethylaluminum [TMA, $Al(CH_3)_3$] exposures at temperatures from 250 to 300 °C. The initial Al_2O_3 films were grown using Al_2O_3 atomic layer deposition (ALD) with TMA and H_2O as the reactants. These Al_2O_3 ALD films are known to be under tensile stress. The progressive decrease in stress-thickness versus Al_2O_3 thermal ALE cycles was consistent with the linear removal of the Al_2O_3 ALD film that contains tensile stress. The results indicated that ALE can be used as a layer removal method to determine the stress distribution in a thin film. The reduction of the stress-thickness by Al_2O_3 thermal ALE at 250, 275, and 300 °C was consistent with the Al_2O_3 etch rates at these temperatures. Surface stresses corresponding to the fluorination and ligand-exchange reactions were also monitored during Al_2O_3 thermal ALE. The TMA reaction resulted in an average negative stress-thickness change of -0.50 ± 0.07 N/m that was consistent with a compressive surface stress. This negative stress-thickness change was attributed to repulsive interactions between surface methyl groups. The subsequent HF reaction then produced a positive stress-thickness change by releasing the compressive stress from the TMA reaction. The fluorination of the initial Al_2O_3 ALD film by HF led to a negative stress-thickness change that was consistent with a gain in compressive stress. The amount of this negative stress-thickness change depended on the thickness of the initial Al_2O_3 ALD film. The average negative stress-thickness change of -0.52 ± 0.08 N/m after >8 Al_2O_3 ALD cycles suggested that the fluorination depth during HF exposure to Al_2O_3 was approximately 9–10 Å.

I. INTRODUCTION

Atomic layer etching (ALE) is a thin film removal process utilizing sequential, self-limiting surface reactions.[1,2] ALE is a useful tool enabling precise control of thin film thicknesses on the Angstrom scale. Most ALE processes employ a surface modification step followed by volatilization of the modified layer.[2,3] For many processes, the modification step is a halogenation reaction. During plasma ALE, the volatilization can be performed by bombardment of energetic ions or atoms for anisotropic etching.[2] During thermal ALE, the volatilization is accomplished using thermally driven reactions that enable conformal, isotropic etching.[1,3] The conformal and isotropic nature of thermal ALE is especially useful for the fabrication of three-dimensional structures used in advanced semiconductor devices.[4,5]

Al_2O_3 ALE is a model thermal ALE system. Many thermal ALE processes have been reported to etch Al_2O_3. The first reported thermal ALE process was Al_2O_3 ALE using hydrogen fluoride (HF) and tin(II) acetylacetonate [$Sn(acac)_2$] as reactants.[6] Subsequent studies demonstrated the etching of Al_2O_3 using HF and trimethylaluminum (TMA).[7,8] Al_2O_3 thermal ALE has also been performed using HF with dimethyl aluminum chloride or BCl_3.[9,10] SF_4 and NbF_5 have also been employed instead of HF for Al_2O_3 thermal ALE.[11,12] All of these chemistries use similar

fluorination and ligand-exchange reactions. The fluorine precursor forms a fluoride surface layer on Al_2O_3.[13–15] The subsequent exposure of the applicable metal precursor undergoes a ligand-exchange reaction with the fluorinated surface and results in the volatilization of the fluorinated layer.[13,16–18]

This study focused on *in situ* measurements of stress in Al_2O_3 films during thermal Al_2O_3 ALE using *in situ* wafer curvature techniques. Stress during thermal ALE is important because stress can cause film damage and feature collapse.[19,20] Stress becomes more important as device sizes become progressively smaller and surface-to-volume ratios become larger. Earlier studies have examined stress during Al_2O_3 atomic layer deposition (ALD) using TMA and H_2O.[21] These *in situ* wafer curvature studies measured both film and surface stress during the TMA and H_2O reactions during Al_2O_3 ALD. The results showed that Al_2O_3 ALD films have tensile stress that ranges with deposition temperature from 508 MPa at 125 °C to 113 MPa at 285 °C.[21] In addition, there were distinct negative stress-thickness changes between −0.2 and −0.6 N/m that were observed during the TMA reactions at temperatures from 125 to 285 °C, respectively. These negative stress-thickness changes were consistent with compressive surface stress. The H_2O reactions then produced equal positive stress-thickness changes that were consistent with the release of the compressive stress.[21]

This paper continues to concentrate on Al_2O_3 with *in situ* stress measurements using wafer curvature techniques during Al_2O_3 thermal ALE. This study focused on Al_2O_3 thermal ALE using HF and TMA as reactants.[7,8] This general process is shown in Fig. 1 and proceeds according to Eqs. (1) and (2),[7]

$$(A)Al_2O_3/Al_2O_3{}^*+6HF \rightarrow Al_2O_3/2AlF_3{}^*+3H_2O, \quad (1)$$

$$(B)Al_2O_3/2AlF_3{}^*+4Al(CH_3)_3 \rightarrow Al_2O_3{}^*+6AlF(CH_3)_2. \quad (2)$$

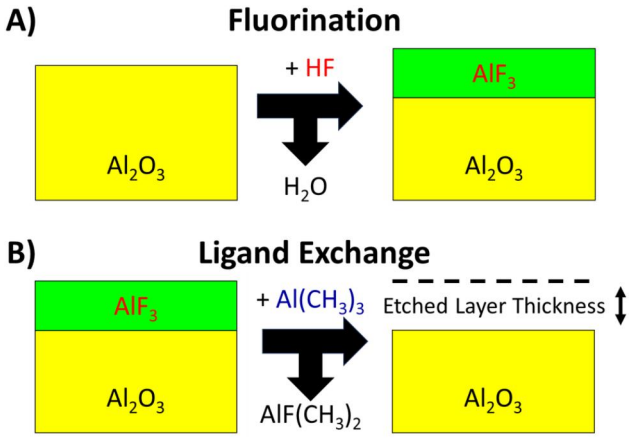

FIG. 1. Sequential fluorination and ligand-exchange reactions for Al_2O_3 thermal ALE using HF and TMA as the reactants. (A) HF reacts with Al_2O_3 to form a fluorinated layer on the surface. (B) AlF_3 is volatilized by ligand exchange with TMA.

The asterisk indicates the surface species during each reaction. Not included in Eqs. (1) and (2) are the individual surface ligands present during these reactions. Each TMA reaction will leave the surface covered in methyl ligands. The HF reaction replaces those methyl ligands with fluorine.

Thermal ALE can be used as a layer removal method to determine the stress distribution in a thin film.[22] The deposition of a stressed layer will cause bending of the underlying substrate. Likewise, the removal of a stressed layer will result in the reversal of the bending. The stress in the removed layer can be calculated based on the change in bending. The stress distribution throughout the film can be determined by sequentially removing layers of the film. The layer removal step has previously been accomplished using a combination of physical machining and chemical etching.[23–25] In addition, ion beam milling has been used for this purpose.[26] ALE can also serve as a layer removal method.

In addition to revealing film stress, Al_2O_3 thermal ALE measurements give insight into the surface stresses that arise during the two sequential reactions that define the Al_2O_3 thermal ALE process. The modification step of the ALE process may potentially lead to large stresses related to volume change associated with the modification of the surface layer of the film. For example, the fluorination of Al_2O_3 to AlF_3 has an estimated volume increase of 226%. This volume increase could lead to a strain of 31% and correspondingly large compressive stress.[27] The volatilization of the fluoride layer by ligand exchange may then be expected to release this compressive stress. The surface ligands produced by the ligand-exchange reaction may also influence the surface stress.

II. EXPERIMENTAL SECTION

The experimental details have been described previously.[21] *In situ* stress measurements were made using wafer curvature techniques and the Stoney equation.[19,28,29] The Stoney equation relates the stress in the film to the curvature of the substrate,[30]

$$\kappa = \frac{1}{R} = \frac{6\sigma_f t_f}{B_s\left(t_s^2\right)} \text{ or } \sigma_f t_f = \frac{\kappa B_s\left(t_s^2\right)}{6}. \quad (3)$$

In Eq. (3), κ is the curvature (1/m), R is the radius of curvature (m), B_s is the biaxial modulus of the substrate (Pa), t_s is the substrate thickness (m), t_f is the film thickness (m), and σ_f is the stress in the film (Pa). The product $\sigma_f t_f$ is the stress-thickness.

A multibeam optical stress sensor (MOSS) from k-Space Associates was used to perform the curvature measurements. The MOSS was used together with a custom, hot wall, radial flow reactor.[21] Nitrogen gas (UHP, 99.999% purity, Airgas) heated to the same temperature as the reactor was used for the carrier gas and backside purge gas. The N_2 carrier gas and reactants were introduced above the center of the sample wafer.[21] A N_2 gas flow also constantly purged the back side of the sample wafer to limit reactant exposure to the top side of the sample.

Sample wafers were double-side polished, 200 μm thick silicon (100) wafers from Seigert Wafer. They had a diameter of 76.2 mm and a p-type resistivity between 1 and 20 Ω cm. The thinner-than-normal wafers were chosen to enhance the sensitivity of the stress measurements. For a given stress and film thickness,

Eq. (3) indicates that the curvature is proportional to $1/(t_s^2)$. A 200 μm thick wafer will have 3.6 times greater curvature for a given film stress than a more common 380 μm thick wafer. For compatibility with the radially symmetric reactor design, the wafers had no flats or notches.

Similar wafer curvature measurements could be performed on 200 or 300 mm wafers. However, there are many experimental complications that arise with larger wafers. Larger wafers are necessarily thicker to support their own weight. Thicker substrates also significantly reduce the curvature resulting from a given stress and film thickness. For larger wafers, wafer warping and other uniformity issues can also be a problem during sample mounting and the MOSS analysis.

Al_2O_3 ALE was performed with HF and TMA as the reactants at temperatures between 250 and 300 °C on Al_2O_3 ALD films.[7,8] The Al_2O_3 film thickness was measured by *ex situ* variable-angle spectroscopic ellipsometry (M2000, J.A. Woollam) before and after Al_2O_3 ALE. These ellipsometry measurements confirmed uniform growth and etch rates over the entire wafer. In addition, the ellipsometry measurements verified that no film growth or etching occurred on the back side of each sample.

The Al_2O_3 ALE pulse sequence was defined by 15 HF mini-doses of 1 s duration. Each mini-dose had a nominal pressure of 0.75 Torr. Each HF mini-dose was separated by a 4 s purge. A 90 s purge followed the conclusion of the HF mini-doses. Subsequently, there were then 15 TMA mini-doses of 1 s duration having a nominal pressure of 0.15 Torr. Each mini-dose was followed by a 4 s purge. Another 90 s purge occurred at the end of the TMA mini-doses.

The Al_2O_3 thin film being etched during the ALE experiments was an Al_2O_3 ALD film. The Al_2O_3 ALD films were deposited using TMA and H_2O as the reactants according to conditions described previously.[21,31] The Al_2O_3 ALD films were deposited on clean silicon wafers that were covered by a native silicon oxide with a nominal thickness of 1.8 nm. All of the etching experiments were performed on Al_2O_3 ALD films grown at 150 °C. This constant deposition temperature kept the initial Al_2O_3 films as consistent as possible and did not introduce variability from the deposition process. The Al_2O_3 ALD films also have higher tensile stresses at lower growth temperatures.[21,32] The Al_2O_3 film thickness was between 20 and 40 nm for the etching experiments.

Fluorination studies were performed at 175 °C. For these studies, at least 50 cycles of an Al_2O_3 ALD film were initially deposited at 175 °C. Subsequent super-cycles were performed with alternating HF exposures and varying numbers of Al_2O_3 ALD cycles to explore the stress from fluorination as a function of the Al_2O_3 ALD film thickness. The HF doses and Al_2O_3 ALD cycles followed the same conditions as described above. The number of Al_2O_3 ALD cycles between HF exposures was varied between 1 and 50 cycles.

All experiments were performed with 180 SCCM of constant N_2 flow for the top-side carrier gas.[21] An additional 1000 SCCM of constant N_2 flow was used as the backside purge.[21] These N_2 flows induce some curvature on the sample wafer. However, this curvature does not affect the results since the flows and induced curvature are constant.

HF vapor for these experiments was obtained from the vapor in equilibrium above liquid HF-pyridine (70 wt. % HF, Sigma-Aldrich). The HF vapor has a pressure of 90–100 Torr and the pyridine partial pressure is negligible.[33] Excess HF was neutralized by bubbling the reactor exhaust through an aqueous calcium oxide solution.

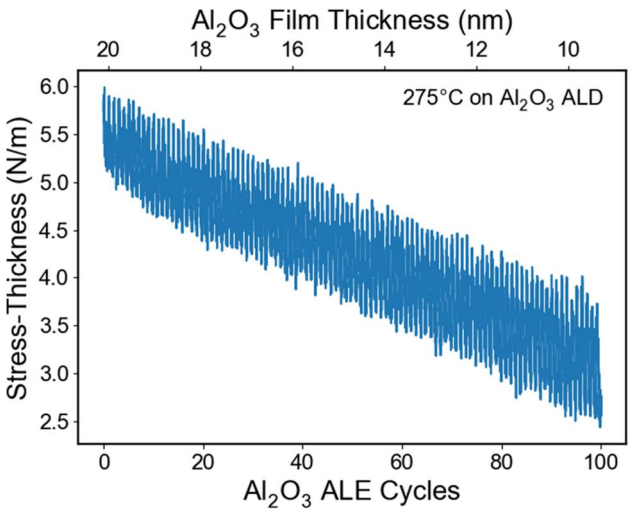

FIG. 2. Stress-thickness during Al_2O_3 thermal ALE at 275 °C. Decrease in stress-thickness corresponds to loss of tensile stress during film removal.

III. RESULTS AND DISCUSSION

A. Film stress during Al_2O_3 ALE

Figure 2 shows the stress-thickness product from the Stoney equation during Al_2O_3 thermal ALE at 275 °C. The stress-thickness is shown as a function of number of ALE cycles. The corresponding Al_2O_3 film thickness is also displayed based on the etch rate for Al_2O_3 thermal ALE. The initial stress-thickness is positive at ~5.7 N/m because the initial Al_2O_3 ALD film is deposited at 150 °C with tensile stress.[21] Previous film stress measurements have demonstrated that the Al_2O_3 ALD film stress is tensile.[21,32] The stress-thickness also grows linearly with the Al_2O_3 ALD film thickness. In contrast, the stress-thickness measured in Fig. 2 during Al_2O_3 thermal ALE decreases linearly with number of ALE cycles corresponding to smaller Al_2O_3 film thicknesses.

If the film stress in the initial film is tensile, then the change in stress-thickness during film removal will be negative. This negative stress-thickness change could be interpreted as a gain in compressive stress. However, this apparent compressive stress corresponds to the removal of the film under tensile stress. The stress-thickness product will change depending on the stress in each layer of the film and whether the film thickness is increasing or decreasing. Table I shows the relationships between the stress-thickness changes corresponding to deposition or etching for tensile and compressive film stress. The stress-thickness change for a film with tensile stress that is being etched will be negative. The stress-thickness change for a film with compressive stress that is being etched will be positive.

TABLE I. Expected stress-thickness changes for films with tensile or compressive film stress depending on whether the film is being grown or etched.

Stress in layer (+ tensile, − compressive)	Film thickness change (+ deposition, − etching)	Stress-thickness change
+	+	+
+	−	−
−	+	−
−	−	+

Stress-thickness measurements made during the ALE process can be used to determine the stress present in the original film prior to the etching. To illustrate ALE as a layer removal method to determine the stress distribution, Fig. 3 shows the stress-thickness for the ALD growth and ALE removal of an Al_2O_3 film. The Al_2O_3 ALD was performed using TMA and H_2O as the reactants at 150 °C. The film was then heated from 150 to 300 °C. Subsequently, the Al_2O_3 thermal ALE was conducted using HF and TMA as the reactants at 300 °C.

The stress-thickness increases linearly versus number of Al_2O_3 ALD cycles during film growth. This behavior was observed in previous *in situ* wafer curvature studies.[21] Increasing values of stress-thickness correspond to tensile stress. For the Al_2O_3 ALD film shown in Fig. 3 at 150 °C, the tensile stress is 354 MPa. Previous measurements obtained a tensile stress of 347 ± 82 MPa for Al_2O_3 ALD films grown at 150 °C.[21,32]

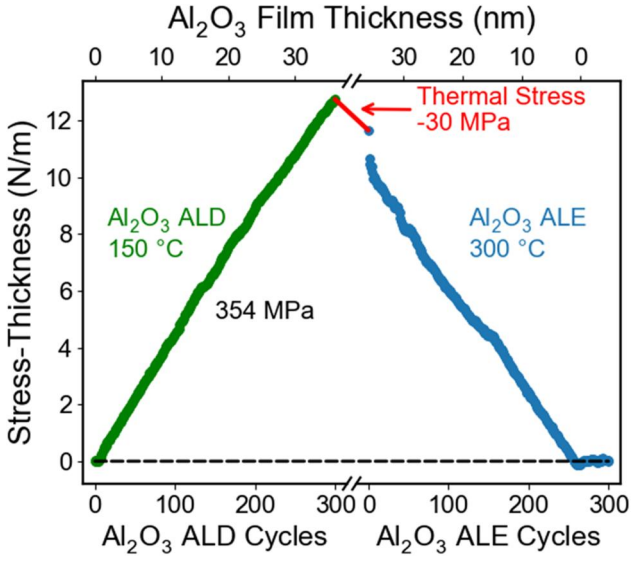

FIG. 3. Stress-thickness for sequential Al_2O_3 ALD at 150 °C and Al_2O_3 thermal ALE at 300 °C. Al_2O_3 ALD displays increasing positive (tensile) stress-thickness. Al_2O_3 ALE is consistent with decreasing the positive stress-thickness. Negative (compressive) stress thickness results from heating film-substrate stack from 150 to 300 °C.

Figure 3 also reveals that raising the temperature from 150 to 300 °C results in a reduction of the stress-thickness and corresponds to a compressive stress. This compressive stress occurs because the Al_2O_3 has a larger coefficient of thermal expansion (CTE) than the silicon substrate.[32] Thermal stress for an Al_2O_3 film on a silicon substrate can be estimated by Eq. (4),

$$\sigma_{\text{thermal}} = \left(\frac{E_{Al_2O_3}}{1-\nu_{Al_2O_3}}\right)(\alpha_{\text{silicon}} - \alpha_{Al_2O_3})\Delta T. \quad (4)$$

The material properties for the thermal stress calculations are $E_{Al_2O_3} = 170$ GPa, $\nu_{Al_2O_3} = 0.24$, and $\alpha_{Al_2O_3} = 4.2\ \frac{\text{ppm}}{°\text{C}}$.[32,34] The silicon CTE, $\alpha_{\text{silicon}} = 3.30\ \frac{\text{ppm}}{°\text{C}}$, is the average silicon CTE between 20 and 300 °C.[35] The CTE mismatch results in 30 MPa of compressive stress. The CTE mismatch reduces the stress in the Al_2O_3 film to 324 MPa upon heating to 300 °C.

The Al_2O_3 ALE then leads to a reduction in the stress-thickness versus Al_2O_3 ALE cycles at 300 °C. Figure 3 reveals that the stress-thickness decreases nearly linearly with Al_2O_3 ALE cycles. The stress-thickness reaches the stress-thickness value prior to the Al_2O_3 ALD after ~270 ALE cycles. The complete removal of stress-thickness corresponds to the entire removal of the Al_2O_3 ALD film. After the Al_2O_3 ALD film is completely removed, the additional Al_2O_3 ALE cycles have no further effect.

The stress in the original Al_2O_3 ALD film can be determined based on the stress-thickness changes during the Al_2O_3 ALE process. The film stress can be calculated by dividing the stress-thickness change by the film thickness change. For the ALE data in Fig. 3, the total stress-thickness change is −11.61 N/m and the total thickness change is −36 nm. Using these values, the calculated stress in the original Al_2O_3 ALD film is 323 MPa of tensile stress. For the Al_2O_3 ALD results in Fig. 3, the tensile stress is 354 MPa.

The difference between 323 MPa from the measurements during Al_2O_3 ALD and 354 MPa from the Al_2O_3 ALE is explained by the thermal stress component because the ALD and ALE occurred at different temperatures. After accounting for the thermal stress component, there is <1% difference between the stress calculated from the Al_2O_3 ALE process and the combined Al_2O_3 ALD and thermal stress. These experiments illustrate that ALE is a viable layer removal method to determine the stress distribution in thin films.

For Al_2O_3 films that have only been partially removed at lower temperatures, the agreement between the stress measured during Al_2O_3 ALD and the stress measured during Al_2O_3 ALE is not as good. For partial etching at higher Al_2O_3 ALE temperatures such as 275 °C, the calculated stress from Al_2O_3 ALE is within 5% of the temperature-adjusted Al_2O_3 ALD stress. At lower etching temperatures, the discrepancy between the stress calculated by Al_2O_3 ALE and the temperature-adjusted Al_2O_3 ALD stress can be as much as 20%.

This larger discrepancy at lower temperatures may be explained by additional stresses present in the partially etched films. These additional stresses may result from surface ligands or from the fluoride layer that may be only partially removed by the ligand-exchange reaction at lower temperatures.[7] These additional

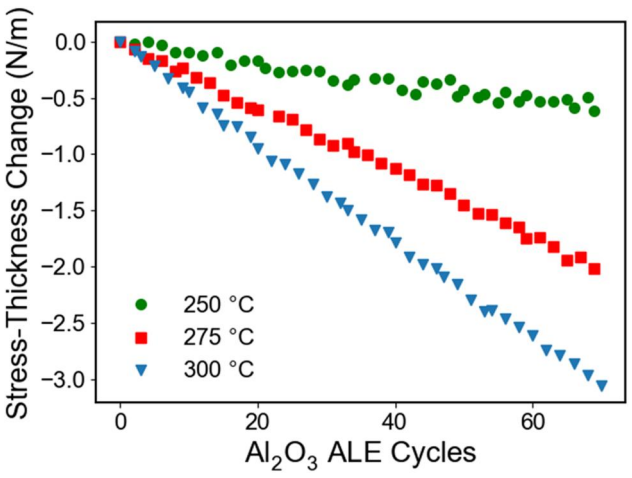

FIG. 4. Stress-thickness change during 70 Al_2O_3 ALE cycles at 250, 275, and 300 °C. Larger change of stress-thickness at higher temperatures is consistent with higher Al_2O_3 etch rate.

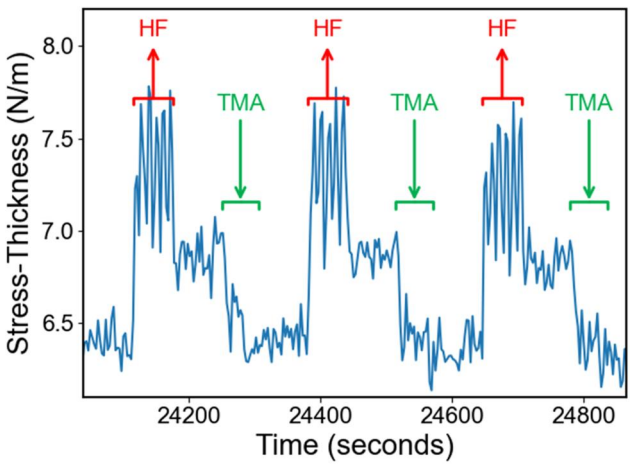

FIG. 5. Stress-thickness vs time for Al_2O_3 ALE performed using sequential HF and TMA reactions at 300 °C. Displayed data correspond to ALE cycles 93, 94, and 95 out of 300 total ALE cycles for stress-thickness results shown in Fig. 3. The brackets show the location of the HF mini-doses and TMA mini-doses in time. TMA reactions produce a negative stress-thickness change (compressive surface stress) and the HF reactions produce positive stress-thickness change (removal of compressive surface stress).

stresses will not be present after the Al_2O_3 film is fully removed by etching leading to the higher accuracy for the fully etched samples.

The slope of the plots of stress-thickness versus number of ALE cycles can be used to estimate the Al_2O_3 etch rate. When the film stress is constant, the stress-thickness change per ALE cycle is equal to the stress times the film thickness change per ALE cycle. The etch rate can be estimated by dividing the slope of the plot of stress-thickness versus ALE cycle by the stress in the film. Figure 4 shows stress-thickness change versus number of Al_2O_3 ALE cycles for various temperatures. As the etching temperature increases from 250 to 300 °C, the slope becomes more negative indicating a larger Al_2O_3 etch rate.

The Al_2O_3 etch rates determined from the stress-thickness changes in Fig. 4 are 0.3, 1.0, and 1.3 Å/cycle at 250, 275, and 300 °C, respectively. The increasing etch rates at higher temperatures are in agreement with previous reports for Al_2O_3 ALE.[7] The TMA ligand-exchange reaction is more favorable at higher temperatures leading to higher etch rates at higher temperatures.[7] Alternatively, if the etch rate is known, the slope of the plot of stress-thickness versus ALE cycles can be divided by the etch rate to calculate the film stress. The Al_2O_3 film stress calculated by this method is within 5% of the temperature-adjusted Al_2O_3 ALD film stress.

B. Surface stress during Al_2O_3 ALE

There are distinct increases and decreases in the stress-thickness shown in Fig. 2 that occur in addition to the linear reduction of the stress-thickness versus number of Al_2O_3 ALE cycles. These increases and decreases appear during each Al_2O_3 ALE cycle. These stress-thickness changes correspond to the HF and TMA surface reactions that are illustrated in Fig. 1.

An expansion of three Al_2O_3 ALE cycles at 300 °C, corresponding to cycles 93, 94, and 95 of the 300 ALE cycles displayed in Fig. 3, is shown in Fig. 5. The brackets indicate the position of the HF mini-doses and TMA mini-doses in time. The HF reaction produces a positive (tensile) stress-thickness change. In addition, the higher pressure HF mini-doses cause the extra positive transients in the stress-thickness that are observed during the duration of the 15 HF mini-doses. The TMA reaction produces a negative (compressive) stress-thickness change. These stress-thickness changes occur on every Al_2O_3 ALE cycle. These stress-thickness changes have an average magnitude of 0.50 ± 0.07 N/m over all etching temperatures.

Figure 6 shows the relationship between stress-thickness and HF and TMA mini-doses during one Al_2O_3 ALE cycle at 300 °C. The manifold pressure was measured by a 100 Torr Baratron® capacitance manometer on the gas manifold. The stress-thickness changes almost immediately on the first several HF and TMA mini-doses. The extra positive transients in the stress-thickness during the HF mini-doses are attributed to the higher pressures during the HF mini-doses that are bending the sample wafer. Pressure increases on the film side of the sample wafer will cause the wafer to bend in the same direction as a tensile stress in the film. The pressure-induced bending is removed when the pressure returns to normal. These pressure-induced effects on the wafer curvature were also observed with inert gas pressure on the film side of the sample wafer.

The apparently periodic oscillations in these positive transients are believed to be a temporal aliasing artifact caused by the time mismatch between the individual HF mini-doses and the curvature measurements. The wafer curvature is sampled at too low a time resolution relative to the individual HF mini-doses to measure the effect of the HF mini-doses on the stress-thickness. The stress-thickness is then constant after the HF and TMA mini-

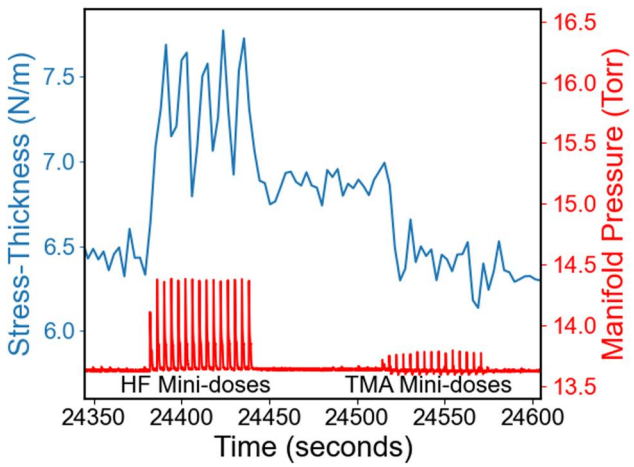

FIG. 6. Relationship between 15 consecutive HF and TMA mini-doses and the stress-thickness during one Al_2O_3 ALE cycle at 300 °C. Positive stress-thickness transients during the HF mini-doses are caused by the HF pressure bending the wafer.

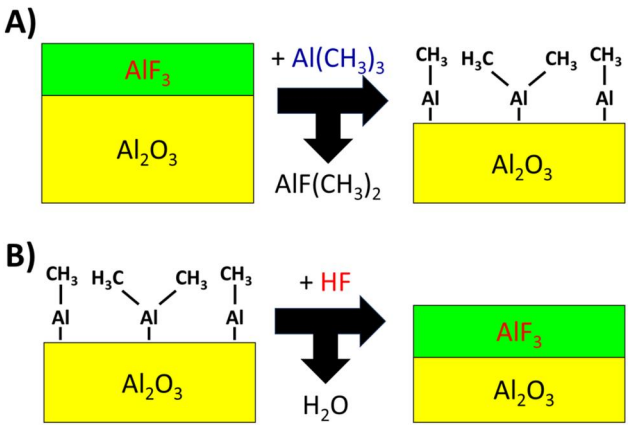

FIG. 7. Surface species present during Al_2O_3 thermal ALE using sequential TMA and HF exposures. (A) TMA reaction removes fluoride layer and leaves the surface terminated by methyl groups. (B) HF reaction removes surface methyl groups and forms a fluoride layer.

doses. The change in surface ligands causing the surface stress is probably complete within the first several HF or TMA mini-doses.

Experimental noise inherent to the curvature measurement can be observed between the HF and TMA exposures in Figs. 5 and 6. This experimental noise is related to local air currents in the laser beam path, vibration of the sample and MOSS instrument, and small pressure variations in the reactor. The most constant conditions exist throughout the purge between the HF and TMA exposures. For *in situ* curvature measurements under these constant conditions, the standard deviation of the curvature is on the order of 5×10^{-5} m^{-1}. This standard deviation equates to a stress-thickness of 0.05 N/m for the 200 μm thick silicon wafers. When averaging over a 90 s purge, the standard error is about 0.01 N/m or about 2% of the average stress-thickness changes measured during Al_2O_3 ALE.

The stress-thickness changes corresponding to the HF and TMA surface reactions during Al_2O_3 ALE are similar to the stress-thickness changes observed during the surface reactions during Al_2O_3 ALD and AlF_3 ALD.[21] For Al_2O_3 ALE, as well as Al_2O_3 and AlF_3 ALD, the TMA reaction results in a negative stress-thickness change that is consistent with compressive surface stress. The TMA reaction during Al_2O_3 ALE results in the volatilization of the fluoride surface layer through the ligand-exchange reaction shown in Fig. 1 and described in Eq. (2). The TMA reaction leaves the surface terminated by methyl groups as displayed in Fig. 7.

Previous FTIR studies have observed the methyl groups on Al_2O_3 surfaces after TMA exposures during Al_2O_3 ALE.[7] The methyl groups are identified by their methyl deformation and stretching vibrations.[7] Repulsive interactions between these methyl groups are believed to cause the negative stress-thickness change.[21] This interpretation is supported by stress measurements during the formation of self-assembled monolayers of alkanethiols on gold surfaces.[36,37] These investigations have observed similar compressive surface stresses that are explained by repulsive interactions between the alkane chains.[36,37]

The following HF reaction then removes the surface methyl groups and forms a fluoride layer as illustrated in Fig. 7. The removal of the methyl groups also removes the compressive surface stress attributed to the methyl groups. This removal of the methyl groups results in a positive (tensile) stress-thickness change. The removal of the methyl deformation and stretching vibrations by the HF reaction has been confirmed by the previous FTIR studies of Al_2O_3 ALE.[7]

Previous quartz-crystal microbalance (QCM) studies of AlF_3 ALD determined that HF is adsorbed on the surface of AlF_3 during AlF_3 ALD at temperatures up to 200 °C.[33] In contrast, previous FTIR studies also observed that there is negligible HF adsorbed on the fluorinated Al_2O_3 surface during Al_2O_3 ALE at ≥250 °C.[7,38] In the absence of adsorbed HF, the main surface species during Al_2O_3 ALE are the methyl groups produced by the TMA reaction. The consistent negative (compressive) stress-thickness changes observed after the TMA reactions during Al_2O_3 ALE, Al_2O_3 ALD, and AlF_3 ALD argue that methyl group interactions are the origin of the compressive surface stress.

C. Evolution of stress during Al_2O_3 ALE

The stress-thickness during the first three Al_2O_3 ALE cycles at 300 °C on the Al_2O_3 ALD film is displayed in Fig. 8. The stress-thickness evolution is qualitatively similar for all Al_2O_3 etching temperatures. The initial fluorination of Al_2O_3 that occurs during the HF exposure in the first half of the first ALE cycle results in a negative stress-thickness change of −0.44 N/m. This negative stress-thickness change indicates a compressive stress. The initial compressive stress is the product of the volume expansion that occurs during the conversion of Al_2O_3 to AlF_3. AlF_3 has a larger molar volume than the corresponding Al_2O_3 and will expand upon conversion.[27,39] A compressive stress arises to counteract

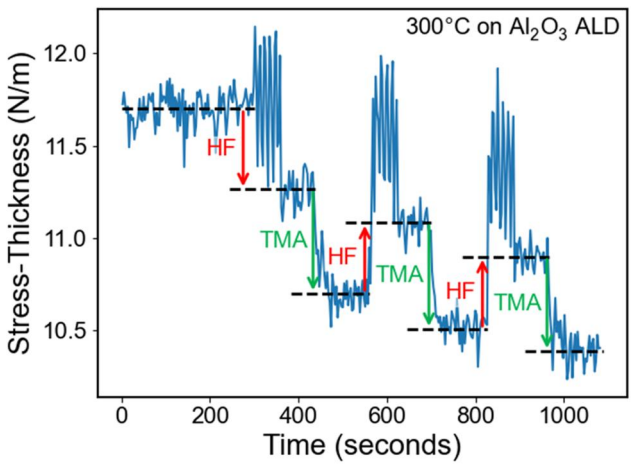

FIG. 8. Evolution of stress-thickness vs time during the first three Al_2O_3 thermal ALE cycles using sequential HF and TMA reactions at 300 °C. Red arrows show net effect of HF reactions while green arrows indicate net effect of TMA reactions.

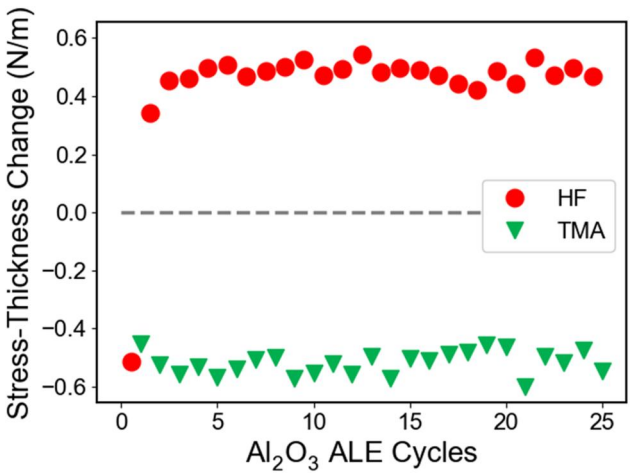

FIG. 9. Stress-thickness changes during sequential HF and TMA reactions at 275 °C. Initial HF reaction results in a negative (compressive) stress-thickness change. First TMA reaction also produces a negative (compressive) stress-thickness change. Subsequent HF and TMA reaction result in alternating positive and negative stress-thickness changes.

this expansion. This negative stress-thickness change may depend on the size of the HF exposure because larger fluoride thicknesses result from higher HF exposures.[15]

The TMA ligand-exchange reaction in the second half of the first ALE cycle also results in a negative (compressive) stress-thickness change of −0.56 N/m. This compressive stress change results from the addition of methyl groups to the surface of the film. The negative stress-thickness change from the initial fluorination is not reversed even though the fluorinated layer has been at least partially volatilized by the ligand-exchange reaction. However, the negative stress-thickness change from the addition of methyl groups may be masking the expected positive stress-thickness change from the loss of the fluorinated layer.

Figure 8 shows that the next HF exposure results in a positive stress-thickness change of 0.38 N/m. This positive stress-thickness change represents a tensile surface stress change corresponding to the removal of surface methyl groups. The negative (compressive) stress-thickness change expected from the additional fluorination of Al_2O_3 may be concealed by the larger positive (tensile) stress-thickness change resulting from the removal of methyl groups.

The next sequential TMA and HF reactions lead to alternation in the stress-thickness changes. The TMA ligand-exchange reactions displayed in Fig. 8 produce negative stress-thickness changes resulting from the addition of surface methyl groups. The HF fluorination reactions then produce positive stress-thickness changes resulting from the removal of the surface methyl groups.

The magnitudes of the surface stress-thickness changes are shown in Fig. 9 for 25 Al_2O_3 ALE cycles at 275 °C. The average stress-thickness change produced by the HF reactions, excluding the first HF reaction that produces compressive stress, is 0.49 ± 0.04 N/m. The average stress-thickness change resulting from the TMA reactions is −0.52 ± 0.04 N/m. The difference between these two average stress-thickness changes is −0.03 N/m. This difference corresponds to the negative stress-thickness change resulting from the etching of the Al_2O_3 ALD film in tensile stress.

The magnitudes of the observed stress-thickness changes in Fig. 9 are comparable with the magnitudes of the surface stresses observed during AlF_3 ALD.[21] AlF_3 ALD is performed with the same HF and TMA reactants but at lower temperatures. The similar magnitude and sign of the surface stress changes for the TMA reactions during Al_2O_3 ALE and AlF_3 ALD argue that the stress-thickness changes during Al_2O_3 ALE are caused primarily by the addition and removal of surface methyl groups.

The TMA reaction is expected to remove at least part of the fluoride layer produced by the HF exposure. Some of the fluoride layer may remain after the TMA exposure. Earlier experiments have detected residual fluorine after the TMA reaction during Al_2O_3 ALE. Previous x-ray photoelectron spectroscopy (XPS),[8] low energy ion scattering (LEIS) measurements,[40] and QCM experiments[7,41] are consistent with some fluorine remaining after the TMA reaction. The amount of residual fluorine is also larger at lower Al_2O_3 ALE temperatures.

The residual fluorine after the TMA exposure may be never fully removed until after the complete removal of the Al_2O_3 film. This residual fluoride film may continue to yield a compressive stress throughout the Al_2O_3 ALE process. In addition, previous experiments have indicated that AlF_3 ALD films contain no film stress.[21] If there is no stress in AlF_3 layers, then the compressive stress observed from the initial fluorination of the Al_2O_3 ALD film may be concentrated in this residual fluoride layer. This residual fluoride layer may be an oxyfluoride layer between Al_2O_3 and AlF_3.

D. Initial stress during HF fluorination of Al_2O_3

Additional studies explored the initial fluorination of Al_2O_3 ALD films. These studies build on previous studies of the

fluorination of Al_2O_3 ALD films by HF.[15,41] In these investigations, Al_2O_3 ALD films were initially deposited on the substrate. Subsequently, the Al_2O_3 ALD films were exposed to HF. The number of Al_2O_3 ALD cycles was varied to change the Al_2O_3 film thickness between HF exposures. These experiments were performed at 175 °C. This temperature was chosen to be below the temperature for Al_2O_3 ALE.[8,38] Consequently, the fluorinated layer is not etched by the TMA in the Al_2O_3 ALD cycle following the HF exposure. In all cases, the Al_2O_3 ALD film was terminated with the H_2O reaction.

Figure 10 shows the stress-thickness change from fluorination as a function of number of Al_2O_3 ALD cycles. For very thin Al_2O_3 films after only a few Al_2O_3 ALD cycles, there is very little negative stress-thickness change from compressive stress resulting from the fluorination. For progressively thicker Al_2O_3 ALD film thicknesses deposited by two to eight Al_2O_3 ALD cycles, the HF exposure fluorinates more Al_2O_3 thickness and produces a larger negative stress-thickness change. After ten or more Al_2O_3 ALD cycles, the HF exposure is not sufficient to fully fluorinate the entire Al_2O_3 layer and the average negative stress-thickness change is constant at -0.52 ± 0.08 N/m.

The constant negative stress-thickness change after eight Al_2O_3 ALD cycles provides a measure of the fluorine penetration depth during HF exposures on Al_2O_3 ALD films. The Al_2O_3 thickness after eight Al_2O_3 ALD cycles corresponds with an Al_2O_3 thickness of ~9–10 Å.[31,42–44] The results in Fig. 10 argue that the fluorine penetration depth into Al_2O_3 ALD films is also about 9–10 Å. Thicker Al_2O_3 layers grown with up to 50 Al_2O_3 ALD cycles all show the same average negative stress-thickness change of -0.52 ± 0.08 N/m from the initial fluorination because the fluorine penetration depth is only 9–10 Å.

The fluorine penetration depth determined from these stress-thickness measurements at 175 °C can be compared with previous studies of the fluorination of Al_2O_3 by HF. Previous XPS investigations based on photoelectron attenuation determined that the fluoride thickness on Al_2O_3 ALD films was approximately 5 Å at 300 °C and HF pressures >4 Torr.[15] Earlier QCM measurements based on mass gains estimated the fluorine penetration depth into Al_2O_3 to be 4.0 Å at 150 °C.[41] This fluorine penetration depth assumed that the Al_2O_3 fluorination exclusively produced AlF_3. The fluorine penetration depth would be larger if the fluorine can also reside in an oxyfluoride layer. Previous LEIS measurements also determined that the fluorine penetration depth in Al_2O_3 extended to 10–15 Å after Al_2O_3 ALE at 350 °C.[8]

The fluorination penetration depth in Al_2O_3 ALD films at 175 °C can be compared with the Al_2O_3 ALE etch rates at 300 °C. The Al_2O_3 ALE etch rate is much smaller on the order of 1 Å/cycle at 300 °C.[7,8] The fluorine penetrates much deeper into the Al_2O_3 film at 175 °C than the Al_2O_3 ALE etch rate at 300 °C. These results suggest that there is a partially fluorinated interfacial layer during Al_2O_3 ALE that is not removed by the TMA ligand-exchange reaction. The previous *in situ* XPS and LEIS studies have confirmed that a residual fluorinated layer exists on Al_2O_3 films after TMA exposures during Al_2O_3 ALE.[8,40] The XPS and LEIS signal intensities after the TMA reaction indicate that the TMA reaction removes less than one-half of the fluorine remaining after the previous HF exposure.[8,40]

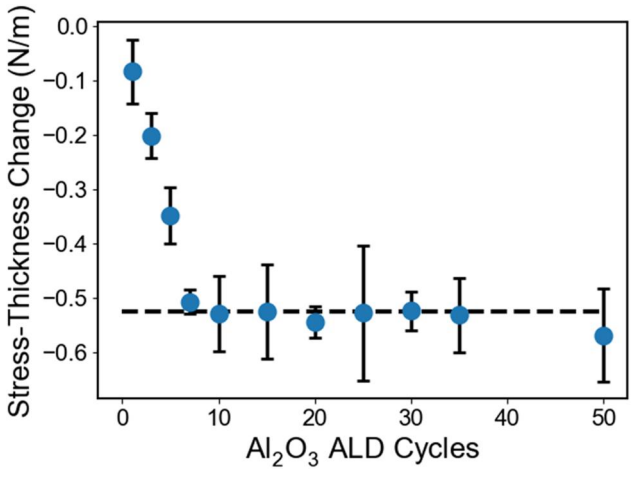

FIG. 10. Stress-thickness change during the initial HF fluorination of Al_2O_3 ALD films grown using variable number of Al_2O_3 ALD cycles.

IV. CONCLUSIONS

Film and surface stress was monitored during Al_2O_3 thermal ALE using *in situ* wafer curvature measurements. The Al_2O_3 thermal ALE was performed using sequential HF exposures for fluorination and TMA exposures for ligand-exchange over the temperature range from 250 to 300 °C. The initial Al_2O_3 films were grown using Al_2O_3 ALD with TMA and H_2O as the reactants at 150 °C. Previous experiments and the results in this study demonstrate that these Al_2O_3 ALD films are under tensile stress.

Measurements of the stress-thickness during Al_2O_3 thermal ALE showed that the positive stress-thickness in the Al_2O_3 ALD films was progressively reduced versus the number of Al_2O_3 ALE cycles. The Al_2O_3 thermal ALE linearly reversed the positive stress-thickness in the original Al_2O_3 ALD film. The entire removal of the Al_2O_3 ALD film produced the complete loss of the positive stress-thickness from the initial Al_2O_3 ALD film. The results illustrate that ALE can be employed as a precise layer removal method to uncover the stress distribution in a thin film.

Knowing the correspondence between stress-thickness changes and Al_2O_3 thin film thicknesses allowed the Al_2O_3 thermal etch rates to be determined using stress-thickness measurements at different temperatures. The stress-thickness changes during Al_2O_3 thermal ALE at 250, 275, and 300 °C yielded Al_2O_3 etch rates of 0.3, 1.0, and 1.3 Å/cycle, respectively. These etch rates are consistent with earlier measurements of these Al_2O_3 etch rates.

The high sensitivity of the *in situ* wafer curvature measurements allowed the surface stresses corresponding to the fluorination and ligand-exchange reactions to be monitored during Al_2O_3 thermal ALE. The TMA reaction resulted in an average negative (compressive) stress-thickness change of -0.50 ± 0.07 N/m that was attributed to repulsive interactions between the surface methyl groups. The following HF reaction then resulted in a positive

(tensile) stress-thickness change that was consistent with the release of the compressive stress from the TMA reaction. The surface stress changes occurred within the first several HF and TMA mini-doses during the Al_2O_3 ALE pulse sequence.

Additional studies explored the fluorination of the initial Al_2O_3 ALD film by HF. Fluorination of the initial Al_2O_3 ALD film consistently produced a negative stress-thickness change corresponding to a compressive stress. This compressive stress is attributed to the volume expansion upon fluorinating Al_2O_3 to AlF_3 or aluminum oxyfluoride. The compressive stresses were dependent on the initial thickness of the Al_2O_3 ALD film. The constant average negative stress-thickness change of -0.52 ± 0.08 N/m after >8 Al_2O_3 ALD cycles indicated that the fluorination depth was approximately 9–10 Å.

ACKNOWLEDGMENTS

This research was supported by Applied Materials. The authors thank Joseph Behnke at Applied Materials for many useful conversations. Additional support was provided by the Superior Energy-Efficient Materials and Device Center (SUPREME), one of the seven centers sponsored by the Semiconductor Research Corporation (SRC) and DARPA under the Joint University Microelectronics Program 2.0 (JUMP 2.0).

AUTHOR DECLARATIONS

Conflict of Interest

The authors have no conflicts to disclose.

Author Contributions

Ryan B. Vanfleet: Formal analysis (lead); Investigation (lead); Writing – original draft (lead); Writing – review & editing (equal). **Victor M. Bright:** Funding acquisition (supporting); Methodology (supporting). **Steven M. George:** Conceptualization (lead); Formal analysis (supporting); Funding acquisition (lead); Methodology (lead); Project administration (lead); Supervision (lead); Writing – review & editing (equal).

DATA AVAILABILITY

The data that support the findings of this study are available within the article.

REFERENCES

[1]A. Fischer, A. Routzahn, S. M. George, and T. Lill, J. Vac. Sci. Technol. A **39**, 030801 (2021).
[2]K. J. Kanarik, T. Lill, E. A. Hudson, S. Sriraman, S. Tan, J. Marks, V. Vahedi, and R. A. Gottscho, J. Vac. Sci. Technol. A **33**, 020802 (2015).
[3]S. M. George, Acc. Chem. Res. **53**, 1151 (2020).
[4]C. T. Carver, J. J. Plombon, P. E. Romero, S. Suri, T. A. Tronic, and R. B. Turkot, ECS J. Solid State Sci. Technol. **4**, N5005 (2015).
[5]W. Lu, Y. Lee, J. C. Gertsch, J. A. Murdzek, A. S. Cavanagh, L. Kong, J. A. Del Alamo, and S. M. George, Nano Lett. **19**, 5159 (2019).
[6]Y. Lee and S. M. George, ACS Nano **9**, 2061 (2015).
[7]Y. Lee, J. W. DuMont, and S. M. George, Chem. Mater. **28**, 2994 (2016).
[8]J. Reif, M. Knaut, S. Killge, M. Albert, T. Mikolajick, and J. W. Bartha, J. Vac. Sci. Technol. A **40**, 032602 (2022).
[9]A. M. Cano, J. L. Partridge, and S. M. George, Chem. Mater. **34**, 6440 (2022).
[10]Y. Lee and S. M. George, J. Phys. Chem. C **123**, 18455 (2019).
[11]J. C. Gertsch, A. M. Cano, V. M. Bright, and S. M. George, Chem. Mater. **31**, 3624 (2019).
[12]V. Sharma, S. D. Elliott, T. Blomberg, S. Haukka, M. E. Givens, M. Tuominen, and M. Ritala, Chem. Mater. **33**, 2883 (2021).
[13]K. Khumaini, G. Cho, H. L. Kim, and W. J. Lee, Surf. Interfaces **72**, 107114 (2025).
[14]S. Kondati Natarajan and S. D. Elliott, Chem. Mater. **30**, 5912 (2018).
[15]A. M. Cano, A. E. Marquardt, J. W. DuMont, and S. M. George, J. Phys. Chem. C **123**, 10346 (2019).
[16]X. Hu and J. Schuster, J. Phys. Chem. C **126**, 7410 (2022).
[17]J. W. Clancey, A. S. Cavanagh, J. E. T. Smith, S. Sharma, and S. M. George, J. Phys. Chem. C **124**, 287 (2020).
[18]A. Lii-Rosales, A. S. Cavanagh, A. Fischer, T. Lill, and S. M. George, Chem. Mater. **33**, 7719 (2021).
[19]G. Abadias *et al.*, J. Vac. Sci. Technol. A **36**, 020801 (2018).
[20]N. T. Eigenfeld, J. M. Gray, J. J. Brown, G. D. Skidmore, S. M. George, and V. M. Bright, Adv. Mater. **26**, 3962 (2014).
[21]R. B. Vanfleet, E. Sortino, A. S. Cavanagh, V. M. Bright, and S. M. George, Appl. Surf. Sci. **724**, 165642 (2026).
[22]*Handbook of Measurement of Residual Stresses*, edited by J. Lu (Fairmont, Atlanta, GA, 1996).
[23]Z. Hu, M. Shao, L. Xiao, H. Pinhui, X. Xu, and Y. Yu, IEEE Trans. Semicond. Manuf. **31**, 514 (2018).
[24]F. Hospers and L. B. Vogelesang, Exp. Mech. **15**, 107 (1975).
[25]D. J. Greving, E. F. Rybicki, and J. R. Shadley, J. Therm. Spray Technol. **3**, 379 (1994).
[26]S. Massl, J. Keckes, and R. Pippan, Acta Mater. **55**, 4835 (2007).
[27]N. Mahuli, A. S. Cavanagh, and S. M. George, J. Vac. Sci. Technol. A **39**, 022403 (2021).
[28]E. Chason and P. R. Guduru, J. Appl. Phys. **119**, 191101 (2016).
[29]E. Chason and B. W. Sheldon, Surf. Eng. **19**, 387 (2003).
[30]G. C. A. M. Janssen, M. M. Abdalla, F. van Keulen, B. R. Pujada, and B. van Venrooy, Thin Solid Films **517**, 1858 (2009).
[31]R. L. Puurunen, J. Appl. Phys. **97**, 121301 (2005).
[32]O. M. E. Ylivaara *et al.*, J. Vac. Sci. Technol. A **40**, 062414 (2022).
[33]Y. Lee, J. W. DuMont, A. S. Cavanagh, and S. M. George, J. Phys. Chem. C **119**, 14185 (2015).
[34]O. M. E. Ylivaara *et al.*, Thin Solid Films **552**, 124 (2014).
[35]J. Thurn and M. P. Hughey, J. Appl. Phys. **95**, 7892 (2004).
[36]R. Berger, E. Delamarche, H. P. Lang, C. Gerber, J. K. Gimzewski, E. Meyer, and H. J. Guntherodt, Science **276**, 2021 (1997).
[37]P. Shrotriya, K. K. S. Karuppiah, R. Zhang, A. Chandra, and S. Sundararajan, Mech. Res. Commun. **35**, 43 (2008).
[38]J. W. DuMont and S. M. George, J. Chem. Phys. **146**, 052819 (2017).
[39]J. A. Murdzek, A. Rajashekhar, R. S. Makala, and S. M. George, J. Vac. Sci. Technol. A **39**, 042602 (2021).
[40]R. Rahman, E. C. Mattson, J. P. Klesko, A. Dangerfield, S. Rivillon-Amy, D. C. Smith, D. Hausmann, and Y. J. Chabal, ACS Appl. Mater. Interfaces **10**, 31784 (2018).
[41]N. Mahuli, A. S. Cavanagh, and S. M. George, J. Vac. Sci. Technol. A **38**, 022407 (2020).
[42]J. W. Elam, M. D. Groner, and S. M. George, Rev. Sci. Instrum. **73**, 2981 (2002).
[43]M. D. Groner, F. H. Fabreguette, J. W. Elam, and S. M. George, Chem. Mater. **16**, 639 (2004).
[44]A. W. Ott, J. W. Klaus, J. M. Johnson, and S. M. George, Thin Solid Films **292**, 135 (1997).